

**Weierstraß-Institut**  
**für Angewandte Analysis und Stochastik**  
**Leibniz-Institut im Forschungsverbund Berlin e. V.**

Preprint

ISSN 0946 – 8633

**The Turing bifurcation in network systems: Collective patterns  
and single differentiated nodes**

Matthias Wolfrum<sup>1</sup>

submitted: January 27, 2012

<sup>1</sup> Weierstrass Institute  
Mohrenstr. 39  
10117 Berlin  
Germany  
E-Mail: [matthias.wolfrum@wias-berlin.de](mailto:matthias.wolfrum@wias-berlin.de)

No. 1675  
Berlin 2012



---

2008 *Physics and Astronomy Classification Scheme*. 89.75Fb, 89.75Kd.

*Key words and phrases.* Turing instability; Diffusively coupled networks; Localized patterns.

Edited by  
Weierstraß-Institut für Angewandte Analysis und Stochastik (WIAS)  
Leibniz-Institut im Forschungsverbund Berlin e. V.  
Mohrenstraße 39  
10117 Berlin  
Germany

Fax: +49 30 2044975  
E-Mail: [preprint@wias-berlin.de](mailto:preprint@wias-berlin.de)  
World Wide Web: <http://www.wias-berlin.de/>

## Abstract

We study the emergence of patterns in a diffusively coupled network that undergoes a Turing instability. Our main focus is the emergence of stable solutions with a single differentiated node in systems with large and possibly irregular network topology. Based on a mean-field approach, we study the bifurcations of such solutions for varying system parameters and varying degree of the differentiated node. Such solutions appear typically before the onset of Turing instability and provide the basis for the complex scenario of multistability and hysteresis that can be observed in such systems. Moreover, we discuss the appearance of stable collective patterns and present a codimension-two bifurcation that organizes the interplay between collective patterns and patterns with single differentiated nodes.

## 1 Introduction

In his seminal work on the chemical basis of morphogenesis [1], A. Turing pointed out that stable equilibria of certain chemical reaction kinetics can destabilize under the influence of a diffusive coupling. In the last decades, this fundamental paradigm for the emergence of dissipative patterns has been applied successfully for the explanation of various phenomena in continuous media, e.g. pigmentation of sea shells, gas discharges, aggregation of bacteria, vegetation patterns and many others. As already mentioned in [1] and later studied in more detail by Othmer and Scriven [2], the same instability mechanism applies not only to continuous diffusive media, but also to the case of discrete units with a diffusive coupling between them, as they can be found e.g. for biological cells [2], chemical reactors [3, 4], or metapopulation dynamics [5, 6].

Dynamics on complex network structures have been studied already extensively in the context of synchronization, see [7, 8] and numerous references therein. In this context however, the main focus is typically on the emergence of uniform behavior of non-uniform units, that are coupled in various, possibly large and heterogeneous network structures. In contrast to that, there are up to now only a few studies on the emergence of non-uniform behavior in networks of identical units. For networks of coupled oscillators the emergence of diffusion-induced instability has been reported in [9]. Earlier studies of activator-inhibitor systems have been mostly restricted to regular networks or networks of small size [4].

Recently, Nakao and Mikhailov studied [10] the emergence of Turing patterns in large irregular networks. Performing extensive numerical simulations for a system with Mimura-Murray reaction kinetics on a large scale-free network, Nakao and Mikhailov demonstrated that in contrast to classical diffusion in continuous media, the Turing instability in such network systems exhibits the following peculiar behavior:

- The emerging stable patterns are very different from corresponding unstable linear modes (in the classical situation, both the modes and the patterns are stationary waves with similar wave numbers).
- There exist stable patterns already before the homogeneous equilibrium undergoes the Turing instability, i.e. the bifurcation is subcritical.
- There is a huge variety of coexisting patterns, showing multistability and hysteresis.

In this paper, we will show that a key to understand these phenomena is the existence of stable localized patterns with single differentiated nodes. In Section 3 we present an analytical approach to solutions with a single differentiated node, that is based on the mean field approximation introduced in [11] and used also in [10]. In this framework we will explicitly calculate the relevant bifurcations and derive conditions for the emergence of such non-homogeneous solutions. In particular, we will show that these specific solutions generically bifurcate subcritically from the homogeneous state, i.e they represent stable patterns that exist before the homogeneous state undergoes the Turing instability. In the following sections we will study a codimension-two bifurcation that reorganizes the solutions with a single differentiated node. In a first step, in Section 4, we will define and localize this bifurcation in the reduced mean-field approximation. Then, in Section 5, we will discuss its implications for the full system and demonstrate in a numerical example that for such parameter values we can indeed observe a supercritical bifurcation of a collective Turing pattern.

We start from a system of the form

$$\dot{u}_i = f(u_i, v_i) + D \sum_{j=1}^N L_{ij} u_j \quad (1)$$

$$\dot{v}_i = g(u_i, v_i) + \sigma D \sum_{j=1}^N L_{ij} v_j \quad (2)$$

The  $N \times N$  matrix  $L$  is the graph-Laplacian of the underlying network with  $N$  nodes, a symmetric matrix with entries  $L_{ij} = 1$  if the nodes  $i$  and  $j$  are connected,  $L_{ij} = 0$  for not connected nodes, and  $L_{ii} = -d_i$ , where the degree  $d_i$  is the number of nodes connected to node  $i$ . The reaction kinetics are given by the nonlinear functions  $f$  and  $g$ . The diffusion constants of both species differ by a factor  $\sigma$ , which is typically used to unfold the Turing bifurcation.

At this point, we do not make any specific assumptions on the structure of the network. As we will see later, our results will be applicable to a rather broad class of networks. In our numerical examples in Sections 3 and 5 we will use a scale free network of rather moderate size ( $N = 20$ ).

As a prototype for a reaction mechanism that displays a Turing instability, we will use the Mimura-Murray kinetics

$$f(u, v) = \frac{au + bu^2 - u^3}{c} - uv \quad (3)$$

$$g(u, v) = uv - v - dv^2 \quad (4)$$

with the default parameter values

$$a = 35, b = 16, c = 9, d = 2/5 \quad (5)$$

as in [10].

## 2 Turing instability

The main feature of the Turing instability is that a stable equilibrium  $(\bar{u}, \bar{v})$  of the reaction kinetics  $\dot{u} = f(u, v)$ ,  $\dot{v} = g(u, v)$  is destabilized by the diffusive spatial interaction. The bifurcation condition can be calculated from a dispersion relation  $\lambda(\beta)$  that is obtained for each fixed value of the bifurcation parameter  $\sigma$  from

$$\det(J_\beta(\bar{u}, \bar{v}) - \lambda \mathbf{Id}) = 0, \quad (6)$$

where

$$J_\beta(\bar{u}, \bar{v}) = \begin{pmatrix} f_u - \beta & f_v \\ g_u & g_v - \sigma\beta \end{pmatrix},$$

and  $f_u, f_v, g_u, g_v$  denote the partial derivatives of the reaction kinetics at the fixed point  $(\bar{u}, \bar{v})$ . Recall that the stability of  $(\bar{u}, \bar{v})$  is reflected by the fact that the eigenvalues  $\lambda(0)$  have negative real part. The onset of Turing instability occurs, when for some  $\sigma = \sigma_T$  a curve of real eigenvalues  $\lambda(\beta)$  touches zero at  $\beta = \beta_T$  from below, which leads to the bifurcation conditions

$$\lambda(\beta_T) = \lambda'(\beta_T) = 0, \quad \lambda''(\beta_T) < 0. \quad (7)$$

In the classical case of diffusion in a continuous medium, the parameter  $\beta_T = \kappa^2 D$  selects the critical wave number  $\kappa$  for a given diffusion length  $D$ . Here, in the same way, for given  $D$  the critical network mode is determined, inserting

$$\beta_T = -\Lambda_c D$$

where  $\Lambda_c$  is the eigenvalue of the graph-Laplacian corresponding to the critical mode. Note that all eigenvalues  $\Lambda$  of the graph-Laplacian are real and negative, except for the zero eigenvalues, corresponding to uniform modes on the connected components of the network. From the bifurcation condition (7) one can derive

$$\sigma_T = \frac{1}{f_u^2} (f_u g_v - 2f_v g_u + 2\sqrt{f_v g_u (f_v g_u - f_u g_v)}) \quad (8)$$

$$\beta_T = \frac{g_v + \sigma_T f_u}{2\sigma_T}, \quad (9)$$

see e.g. [10]. In particular, for any nontrivial network mode with network eigenvalue  $\Lambda$ , we can adjust  $D = -\beta_T/\Lambda$  such that this network mode destabilizes exactly at the Turing point  $\sigma = \sigma_T$ .

In the following, we will assume that for the reaction kinetics  $f, g$  there is a stable equilibrium  $(\bar{u}, \bar{v})$  and positive values  $\sigma = \sigma_T$  and  $\beta = \beta_T$  at which  $(\bar{u}, \bar{v})$  undergoes a supercritical Turing bifurcation. For the Mimura-Murray kinetics (3)–(4) with the parameters (5) this occurs for the equilibrium  $(\bar{u}, \bar{v}) = (5, 10)$  at  $\sigma_T \approx 15.507$ ,  $\beta_T \approx 1.5377$ .

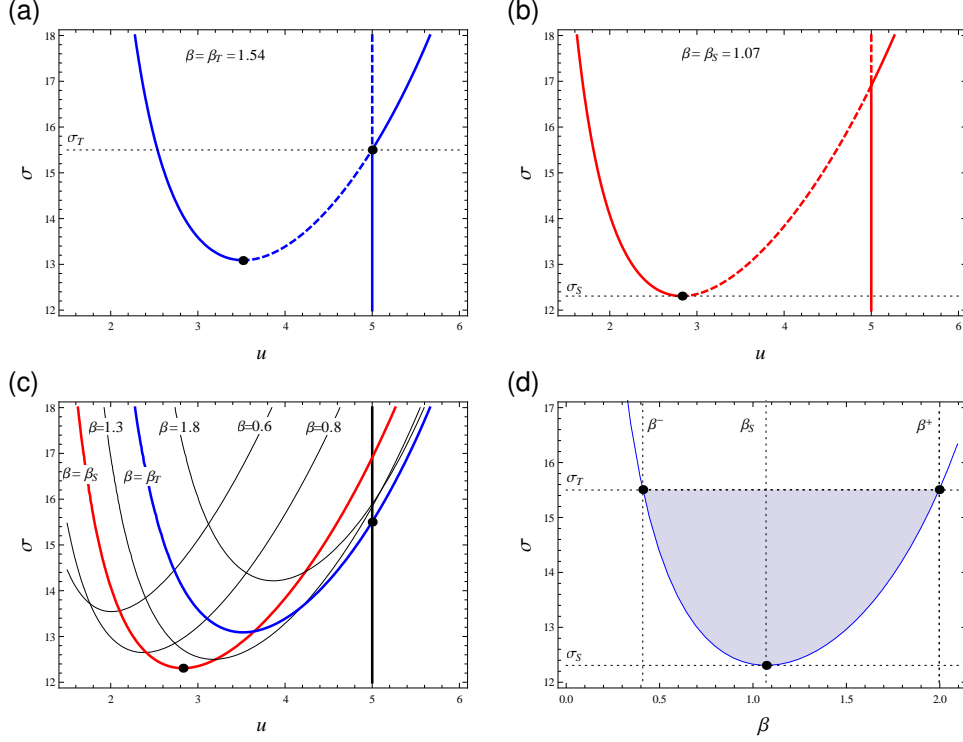


Figure 1: Stationary solutions of system (10)–(11) with reaction kinetics given by (3)–(5) and varying parameter  $\sigma$ . (a) For  $\beta = \beta_T \approx 1.54$  transcritical bifurcation at the Turing instability  $\sigma_T$  and fold. (b) For  $\beta = \beta_S \approx 1.08$  the fold occurs at the minimal value  $\sigma_S$ . (c) For other values of  $\beta$  both the fold and the transcritical bifurcation occur for values of  $\sigma$  larger than  $\sigma_T$  and  $\sigma_S$ , respectively. (d) Fold curve in the  $(\beta, \sigma)$ -plane; region between fold curve and  $\sigma = \sigma_T$  (shaded), where stable SDN-solutions can be expected.

### 3 Dynamics of a single node

We consider now the dynamics of a single node  $(u_k, v_k)$  under the assumption that all other nodes are fixed at the stable equilibrium of the reaction kinetics

$$(u_i, v_i) = (\bar{u}, \bar{v}) \text{ for all } i = 1, \dots, N, i \neq k.$$

Inserting this into the equations (1)–(2) we obtain the single node system

$$\dot{u}_k = f(u_k, v_k) + \beta(\bar{u} - u_k) \quad (10)$$

$$\dot{v}_k = g(u_k, v_k) + \sigma\beta(\bar{v} - v_k). \quad (11)$$

The parameter  $\beta$ , which is given by  $\beta = d_k D$ , where  $d_k$  is the degree of the network node  $k$ , will be used as an additional bifurcation parameter; in this way we can trace the behavior of nodes with varying degree within a single network. The system (10)–(11) coincides with the mean field approach from [11] applied to the homogeneous solution and we will discuss below its relevance for the full network dynamics.

In a first step, we study the fixed points of system (10)–(11) and their stability. Obviously, the fixed point of the reaction kinetics  $(u_k, v_k) = (\bar{u}, \bar{v})$  is a fixed point of this system, independent on the choice of the parameters  $\beta$  and  $\sigma$ . Its stability is again determined by (6). Note that the stability of  $(\bar{u}, \bar{v})$  that we assumed for  $\beta = 0$  is retained for  $\sigma = 1$  and all  $\beta > 0$ . For increasing  $\sigma$  the condition (7) indicates the appearance of a zero eigenvalue  $\lambda(\beta)$  at  $\sigma = \sigma_T$  and  $\beta = \beta_T$ . Due to the fact that the equilibrium  $(\bar{u}, \bar{v})$  does not depend on the bifurcation parameter  $\sigma$ , this zero eigenvalue leads here generically to a transcritical bifurcation (cf. Figure 1(a)). According to (7), there are values of  $\beta$  with  $\lambda(\beta) = 0$  also for  $\sigma > \sigma_T$  inducing further transcritical bifurcations for values  $\beta$  different from  $\beta_T$ . The corresponding values of  $\sigma$  can (locally) be written as a function  $\sigma_{TC}(\beta)$ , which attains its minimal value  $\sigma_T$  exactly at  $\beta_T$  (cf. Figure 1(c)).

Now we study the branch of stationary solutions bifurcating from the branch  $(u_k, v_k) = (\bar{u}, \bar{v})$  in the transcritical bifurcation. For given reaction kinetics, e.g. (3)–(5), it can be easily computed numerically. Figure 1(a) shows the typical situation, where the part of the branch that emanates unstable from the transcritical bifurcation undergoes a saddle-node (fold) leading to a further branch of stable stationary solutions with  $(u_k, v_k) \neq (\bar{u}, \bar{v})$ . The condition for this saddle-node bifurcation is that at an equilibrium  $(u_k, v_k) \neq (\bar{u}, \bar{v})$  the matrix  $J_\beta(u_k, v_k)$  has an eigenvalue  $\lambda(\beta) = 0$ . Varying now the parameter  $\beta$  (cf. Figure 1(c)), this fold will appear for varying values of  $\sigma$ . For the emergence of patterns in the original network system (1)–(2) with increasing main bifurcation parameter  $\sigma$ , the minimal value  $\sigma = \sigma_S$  at which this fold can occur will be of particular importance (cf. Figure 1(b)). The corresponding bifurcation condition is given by

$$\lambda(\beta_S) = \lambda'(\beta_S) = 0, \quad (12)$$

where  $\lambda(\beta)$  is the leading eigenvalue of the matrix  $J_\beta(u, v)$ , evaluated at a fixed point  $(u_k, v_k) \neq (\bar{u}, \bar{v})$  of system (10)–(11). Note that the corresponding value  $\beta_S$  is in general different from  $\beta_T$  and the corresponding value  $\sigma_S$  is smaller than  $\sigma_T$ .

In Figure 1(d) we present the fold curve for parameters  $\beta$  and  $\sigma$ , using the reaction kinetics (3)–(5). Since  $\sigma_S \leq \sigma_T$ , we can also find values  $\beta^-, \beta^+$ , with  $\beta^- \leq \beta_S \leq \beta^+$ , where the fold curve crosses the line  $\sigma = \sigma_T$ , see Figure 1(d). Together with  $\sigma_S$ , these values will play an essential role when we will use now the stable stationary solutions of system (10)–(11) to describe certain stable stationary solutions of the full network system (1)–(2).

A stationary solution of system (1)–(2) where only one single node attains a value substantially different from  $(\bar{u}, \bar{v})$ , while all other nodes stay close to the homogeneous solution  $(\bar{u}, \bar{v})$  will be called *single-differentiated-node* solution (SDN-solution). We will now discuss, under which conditions a stable stationary solutions of system (10)–(11) can be used to describe a stable SDN-solution for the full system (1)–(2). The assumption that the deviation of a single node induces only a small deviation to all other nodes, that we used to derive system (10)–(11), is asymptotically true in large networks with large average degree. Hence, by the implicit function theorem the existence of SDN-solutions close to hyperbolic stationary solutions of system (10)–(11) holds in an asymptotic sense in sufficiently large networks.

For the stability of a corresponding SDN-solution, we need in addition to the stability of the approximating solution in system (10)–(11), that accounts for perturbations at the differentiated node, also stability with respect to perturbations of the remaining nodes, which in system (10)–

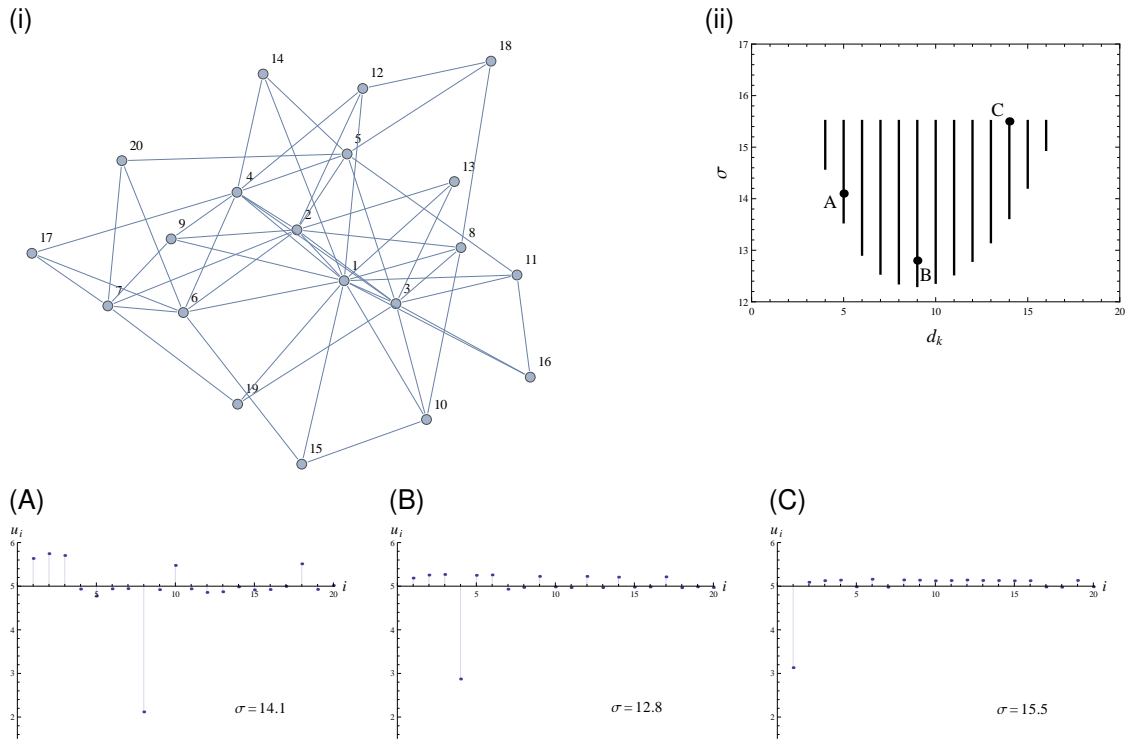


Figure 2: (i) Example of a scale-free network with 20 nodes. Degrees (14, 10, 10, 9, 7, 7, 6, 5, 4, 4, 4, 4, 3, 3, 3, 3, 3, 3, 3, 3). (ii) Coexisting branches of stable SDN-solutions of the full system with differentiated nodes of varying degree  $d_k$ , predicted for fixed  $D = 0.12$  by the single-node system (10)–(11). Examples of numerically calculated stable SDN-solutions for system (1)–(5) using the network given in (i) with various choices of  $\sigma$  and degrees  $d_k$  of the differentiated node that are indicated by dots in panel (ii): (A)  $d_k = 5$  and  $\sigma = 14.1$ ; (B)  $d_k = 9$  and  $\sigma = 12.8$ ; (C)  $d_k = 14$  and  $\sigma = 15.5$ .

(11) are clamped to  $(\bar{u}, \bar{v})$ . This stability is described, again in an asymptotic sense, by the stability of the uniform stationary solution  $(u_i, v_i) = (\bar{u}, \bar{v})$  in the complementary system

$$\dot{u}_i = f(u_i, v_i) + D \sum_{j=1, j \neq k}^N L_{ij} u_j \quad (13)$$

$$\dot{v}_i = g(u_i, v_i) + \sigma D \sum_{j=1, j \neq k}^N L_{ij} v_j \quad (14)$$

with  $i = 1, \dots, N, i \neq k$ . This stability will be lost at the Turing point  $\sigma = \sigma_T$ , if the complementary network has an eigenvalue  $\Lambda = -D/\beta_T$ . In this way, we obtain that the stable branch emanating directly from the transcritical bifurcation will in general not give rise to stable SDN-solutions of the full network, but only the stable part beyond the fold of the other branch, that lies below  $\sigma_T$  (shaded region in Figure 1(d)). For fixed  $\sigma \in (\sigma_S, \sigma_T)$  solutions for all values of  $\beta$  above the fold curve can lead to coexisting stable SDN-solutions of the full network with differentiated nodes of corresponding degree  $d_k = \beta/D$ , as soon as in a sufficiently large network a node with this degree is available. In particular in a scale free network, where the degree distribution extends over a broad range, and choosing a small diffusivity  $D$  this leads to a large number of coexisting stable SDN-solutions. However, nodes with degree  $d_k$  not in the interval  $(\beta^-/D, \beta^+/D)$  can never be differentiated in a stable SDN-solution. In Figure 2(ii) we show the resulting branches of coexisting stable SDN-solutions with different degrees that can appear in the full system for fixed  $D = 0.12$  as soon as a node with the corresponding degree is available. Using the example network given Figure 2(i) we have calculated numerically some stable SDN-solutions, that are displayed in Figure 2(A)–(C). It turns out that already in this rather small network, we get a reasonably good prediction from the single-node system (10)–(11). Note that for increasing degree of the differentiated node, the solution for the full system comes closer to that predicted by the single-node system.

A further consequence of our analysis is that the bifurcations at the two ends of each branch of SDN-solutions are of a genuinely different nature. At the lower point, given by the fold curve, the bifurcation takes place in a mode that is localized at the differentiated node, whereas the destabilization at  $\sigma_T$  involves a collective mode of the full network.

## 4 A codimension two bifurcation in the single node system

In the previous section, we investigated the appearance of stable SDN-solutions in a generic situation. Comparing the results with the classical Turing bifurcation in continuous systems, we find two striking differences:

- The stable SDN-solutions appear for  $\sigma < \sigma_T$ , i.e. in a subcritical scenario, even though the same reaction kinetics induce a supercritical Turing bifurcation in a continuous medium.
- The bifurcation diagrams show an asymmetry: in a stable SDN-solution, the differentiated nodes take values only at one side of the homogeneous equilibrium. In our example,  $u_k < \bar{u}$  and  $v_k < \bar{v}$ .

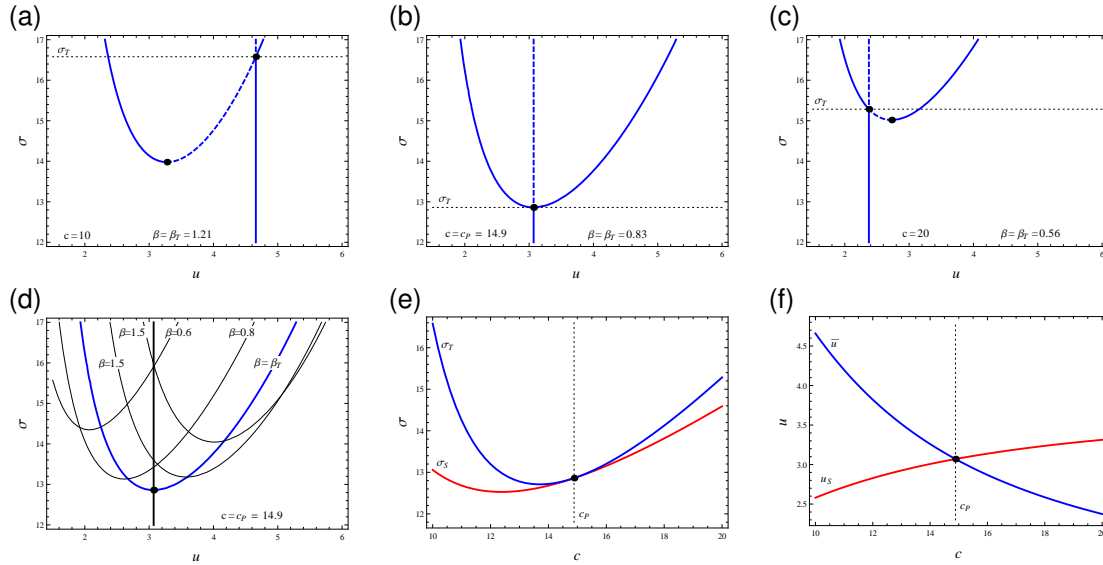


Figure 3: Stationary solutions of system (10)–(11). Varying the parameter  $c$  in the reaction kinetics the generic transcritical bifurcation at  $\sigma_T$  degenerates to a pitchfork bifurcation (other parameters  $a = 25$ ,  $b = 15$ ,  $d = 0.5$ ): (a) For  $c < c_P$  the fold point is to the left of the transcritical point; (b) For  $c = c_P$  the fold point coincides with the transcritical point, inducing a pitchfork; (c) For  $c > c_P$  the fold point is to the right of the transcritical point. (d) Fixed  $c = c_P$  and varying  $\beta$ : pitchfork at  $\beta = \beta_T$  (blue curve) and transcritical for other values of  $\beta$  (black curves). (e) Appearance of stable SDN-solutions  $\sigma_S$  and onset of Turing instability  $\sigma_T$  for varying parameter  $c$ ; both values satisfy  $\sigma_S \leq \sigma_T$  and coincide at the pitchfork bifurcation  $c = c_P$ . (f)  $u$ -values  $u_S$  of the first stable differentiated node appearing for  $\beta = \beta_S$  at  $\sigma_S$  and  $\bar{u}$  of the homogeneous solution for varying parameter  $c$ ; both values cross at the pitchfork bifurcation  $c = c_P$ .

We will now show that these properties are organized by a codimension-two bifurcation that is specific for the Turing bifurcation in networks. Recall that the transcritical bifurcation occurs generically in the single node system (10)–(11), when the homogeneous equilibrium loses its stability at the Turing point. Including now a secondary parameter in addition to the Turing parameter  $\sigma$  and following the branch of transcritical bifurcations in these two parameters, we can generically meet the situation where the transcritical bifurcation degenerates into a pitchfork bifurcation. We could try to find a pitchfork bifurcation by varying the parameter  $\beta$  in the single node system. But this pitchfork will then occur generically at some  $\beta_P \neq \beta_T$  and hence  $\sigma_P$  will be bigger than  $\sigma_T$ . But as we argued above, solutions of the single node system with  $\sigma > \sigma_T$  cannot be stable in the full network. In order to obtain the pitchfork bifurcation at the stability boundary of the homogeneous solution of the full network, we have to use a parameter of the reaction kinetics as the second bifurcation parameter, and fix  $\beta$  at  $\beta_T$ . Note that varying the parameters of the reaction kinetics, the position of the homogeneous equilibrium  $(\bar{u}, \bar{v})$  will vary and hence, according to (8) and (9), also the values of  $\sigma_T$  and  $\beta_T$ .

Since this is a bifurcation of the stationary solutions only, the parameter value of the bifurcation can be determined in general by a Lyapunov-Schmidt procedure. In the example (3)–(4), it can even be reduced to a one dimensional problem, avoiding extra technicalities. The fixed point of the reaction kinetics  $(\bar{u}, \bar{v})$  satisfies

$$\bar{u}^2 + \left(\frac{c}{d} - b\right) \bar{u} - \frac{c}{d} - a = 0 \quad (15)$$

$$\bar{v} = \frac{\bar{u} - 1}{d}. \quad (16)$$

Similarly, in the system for the fixed points of (10) with (3) we find

$$v = \beta \left(\frac{\bar{u}}{u} - 1\right) + \frac{a + bu - u^2}{c} \quad (17)$$

In the remaining fixed point equation from (11) and (4)

$$v(u - 1 - dv) + \sigma\beta(\bar{v} - v) = 0, \quad (18)$$

we can use (17) and (16) to eliminate the unknown variables  $v$  and  $\bar{v}$ . The result is a scalar equation of the form

$$\mathcal{F}(u, \bar{u}) = 0. \quad (19)$$

that determines the fixed points of system (10)–(11) for given values of  $\beta$  and  $\sigma$  and a solution  $\bar{u}$  of equation (15). This function has a double root both at the fold and at the transcritical bifurcation discussed above. The pitchfork is characterized by

$$\partial_{uu}\mathcal{F}(u, \bar{u}) = 0. \quad (20)$$

Finally, we insert  $\sigma = \sigma_T$  and  $\beta = \beta_T$  from (8) and (9), and  $u = \bar{u}$  to localize the pitchfork at the Turing point. In this way, the bifurcation condition (20) involves only the coordinate  $\bar{u}$  of the pitchfork point and the parameters of the reaction kinetics  $a, b, c, d$ . Together with (15) it can be used to solve for the bifurcation point that turns out to be of codimension one with respect to the

reaction parameters  $a, b, c, d$ . A second codimension was already introduced by the condition  $\sigma = \sigma_T$  that we made above. Note that equation (19) is trivially satisfied for  $u = \bar{u}$  and does not induce an extra bifurcation condition.

In Figure 3 we have illustrated the bifurcation scenario for the example (3)–(4). We have chosen here the parameter  $c$  to unfold the pitchfork bifurcation and slightly adapted the other parameters in order to avoid a Hopf instability of the equilibrium  $(\bar{u}, \bar{v})$ . Panels (a)–(c) show the fixed points of system (10)–(11) for varying  $\sigma$  and parameter values  $c$  before, in the moment, and after the bifurcation. Note that in all three plots we have adjusted  $\beta = \beta_T$ , that has to be determined from (9) for varying  $c$ . Panel (d) shows that at the pitchfork bifurcation  $c = c_P$  even for varying  $\beta$  there exist no SDN-solutions for  $\sigma < \sigma_T$  and hence the SDN-solutions are all unstable. This corresponds to the fact that due to our bifurcation condition, the emergence of SDN-solutions at  $\sigma_S$  coincides here with the onset of Turing instability, i.e. we have  $\sigma_T = \sigma_S$  (see panel (e)). Finally, panel (f) illustrates that the differentiated node, when appearing in the minimal fold at  $\sigma_S$ , takes a value  $u_S$  that switches to the other side of  $\bar{u}$  in the moment of the pitchfork bifurcation. This holds true not only for this specific solution, but also for all other stable SDN-solutions. In contrast to the solution from the minimal fold, they disappear not only directly at the point of bifurcation, but are absent (i.e. above  $\sigma_T$ ) for an open interval of parameters  $c$  around the bifurcation point  $c_P$ .

## 5 The full system at the pitchfork bifurcation: supercritical emergence of a collective pattern

In the previous section we showed that at the pitchfork bifurcation, the single-node system (10)–(11) does not indicate the existence of stable SDN-solutions. In particular, there are no such solutions before the onset of the Turing instability at  $\sigma_T$ . Hence, we can expect in this situation a supercritical bifurcation of a collective pattern, i.e. a pattern given by the mode corresponding to the critical eigenvalue of the graph-Laplacian of the network.

In Figure 4 we show the results of corresponding numerical calculations. As the underlying network, we took again the scale-free network given Figure 2(i). Panel (a) of Figure 4 shows that the homogeneous solution loses its stability in a pitchfork bifurcation, giving rise to two branches of stable collective patterns. Note that the location of this pitchfork bifurcation of the full system has been predicted in the previous section without taking into account the specific structure of the network that has been used here.

Panel (b) of Figure 4 shows the critical linear mode at the instability that is given by an eigenmode of the graph-Laplacian. Panels (c) and (d) show the stable nonlinear patterns at the two instances A and B indicated in panel (a), representing a short and a longer distance from the point of bifurcation. Note that in contrast to the SDN-solutions, these patterns do not show any preferred direction of differentiation. Obviously, each individual node differentiates in opposite directions on the upper and lower branch, respectively.

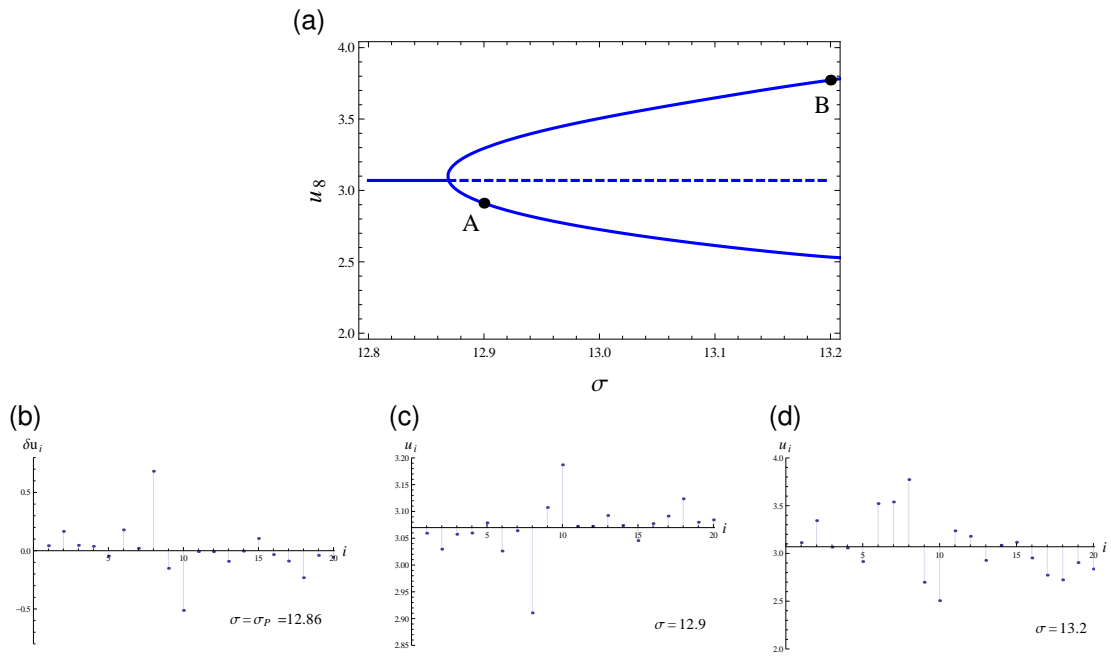


Figure 4: Supercritical bifurcation of a collective Turing pattern for increasing parameter  $\sigma$ ; network as in Fig 2(i), other parameters:  $a = 25$ ,  $b = 15$ ,  $c = 14.9$ ,  $d = 0.5 D = 0.12$ . (a) numerically calculated branches of bifurcating solutions, stable (solid) and unstable (dashed); (b) critical linear network mode; (c) stable stationary solution for  $\sigma = 12.9$  (A); (d) stable stationary solution for  $\sigma = 13.2$  (B).

## 6 Conclusions

In this paper we investigated the emergence of differentiation patterns in diffusively coupled networks with activator-inhibitor kinetics. In comparison to continuous media, such systems with irregular heterogeneous networks show a wealth of interesting and unexpected phenomena that require new mathematical techniques [12]. We have demonstrated in this paper that in such systems close to the onset of Turing instability there can exist two different types of stable patterns. There are stable stationary solutions with single differentiated nodes (SDN-solutions) and collective patterns that emerge from destabilizing eigenmodes of the network. The solutions with single differentiated nodes appear typically in a subcritical bifurcation scenario, i.e. before the homogeneous equilibrium loses its stability in a Turing bifurcation.

SDN-solutions, their stability, and their bifurcations have been studied in a reduced system obtained by a mean-field approach. In particular, we showed how their competition with the collective modes is organized in a codimension-two bifurcation of pitchfork type.

In sufficiently large networks, our results allow also to infer on the existence of stable solutions with several differentiated nodes that are localized such that their neighborhoods do not overlap to much. In this way, the SDN-solutions can be considered as the basic building blocks for a huge amount of coexisting stable solutions. The resulting complex spatial behavior can be understood as a specific form of spatial chaos, that has been described before in regular networks (see [13, 14, 15]). Our results apply for a wide class of large heterogeneous networks. As particular examples, we considered scale-free networks. Due to their wide degree-distribution, they demonstrate the differences to systems in continuous media, or their discretizations, in a prominent way.

Whereas Turing patterns in continuous media are characterized by their wave number, the patterns in heterogeneous networks are characterized by the degrees of the nodes that take part in the differentiation. For the collective modes, it is known that the corresponding eigenmodes of the graph-Laplacian for scale-free networks are concentrated mainly on nodes of a characteristic degree, that is proportional to the eigenvalue [16]. For the SDN-solutions, we calculated the degree of the differentiated node at the onset of their existence and the growing range of degrees that allow for differentiation in the course of the bifurcation. It turns out that, in general, the characteristic degree of the eigenmode of the Turing bifurcation differs from the degree that is prevalent for the SDN-solutions. This adds another aspect to the complex interplay between localized and collective patterns.

In this paper, we have focused our attention to the stable patterns appearing at the onset of Turing instability. Numerical observations in [10] indicate that there is an interesting transition from this regime to the patterns that develop far from bifurcation. However, these more complex patterns seem to be not accessible by the mainly analytical approach presented in this paper. Instead, a numerical bifurcation analysis could possibly reveal further interesting phenomena.

## References

- [1] A. M. Turing. The chemical basis of morphogenesis. *Philosophical Transactions of the Royal Society of London. Series B, Biological Sciences*, 237(641):37 – 72, 1952.
- [2] H.G. Othmer and L.E. Scriven. Instability and dynamic pattern in cellular networks. *J. Theor. Biol.*, 32:507–537, 1971.
- [3] Werner Horsthemke, Kwan Lam, and Peter K. Moore. Network topology and turing instabilities in small arrays of diffusively coupled reactors. *Physics Letters A*, 328:444–451, 2004.
- [4] Peter K. Moore and Werner Horsthemke. Localized pattern in homogeneous networks of diffusively coupled reactors. *Physica D*, 206:121–144, 2005.
- [5] I. Hanski. Metapopulation dynamics. *Nature*, (396):41 – 49, 1998.
- [6] Vittoria Colizza, Romualdo Pastor-Satorras, and Alessandro Vespignani. Reaction-diffusion processes and metapopulation models in heterogeneous networks. *Nature Physics*, 3:276–282, 2007.
- [7] A. Pikovsky, M. Rosenblum, and J. Kurths. *Synchronization. A Universal Concept in Non-linear Sciences*. Cambridge University Press, 2001.
- [8] S. Boccaletti, V. Latora, Y. Moreno, M. Chavez, and D.-U. Hwang. Complex networks: Structure and dynamics. *Physics Reports*, 424:175–308, 2005.
- [9] Alexander S. Mikhailov Hiroya Nakao. Diffusion-induced instability and chaos in random oscillator networks. *Physical Review E*, 79:036214/1–036214/5, 2009.
- [10] H. Nakao and A.S. Mikhailov. Turing patterns in network-organized activator-inhibitor systems. *Nature Physics*, (6):544 –550, 2010.
- [11] Romualdo Pastor-Satorras and Alessandro Vespignani. Epidemic spreading in scale-free networks. *Physical Review Letters*, 86(14):3200–3203, 2001.
- [12] Romualdo Pastor-Satorras and Alessandro Vespignani. Pattern of complexity. *Nature Physics*, 6:480–481, 2010.
- [13] Shui-Nee Chow, John Mallet-Paret, and Erik S. Van Vleck. Dynamics of lattice differential equations. *Int. J. Bifurcation Chaos Appl. Sci. Eng.*, 6(9):1605–1621, 1996.
- [14] L.P. Nizhnik, I.L. Nizhnik, and M. Hasler. Stable stationary solutions in reaction-diffusion systems consisting of a 1-d array of bistable cells. *International Journal of Bifurcation and Chaos*, 12(2):261–279, 2002.
- [15] Iryna Omelchenko, Yuri Maistrenko, Philipp Hövel, and Eckehard Schöll. Loss of coherence in dynamical networks: Spatial chaos and chimera states. *Phys. Rev. Lett.*, 106:234102, Jun 2011.

- [16] Patrick N. McGraw and Michael Menzinger. Laplacian spectra as a diagnostic tool for network structure and dynamics. *Phys. Rev. E*, 77:031102, Mar 2008.